J Mater Sci (2011) 46:7184–7190
DOI 10.1007/s10853-011-5554-0

SIZE DEPENDENT EFFECTS

Model calculation of the effectiveness of Tb^{3+} containing glass as a wavelength converter in thin film solar cells

M. Sendova-Vassileva

Received: 13 December 2010 / Accepted: 8 April 2011 / Published online: 21 April 2011

Abstract Wavelength converters have been proposed as one of the ways to achieve higher efficiency in third generation solar cells. The idea is to shift the wavelength of the light absorbed by the solar cell to the spectral region where the device is most efficient. Higher energy photons are often absorbed unproductively near the front contact of the solar cells. By the application of photoluminescent materials these photons are transformed into longer wavelength ones, which contribute more effectively to the generated photocurrent. In this study the improvement that a wavelength converter containing Tb^{3+} ions can produce on the efficiency of a thin film silicon single junction solar cell under AM 1.5 solar radiation is assessed by model calculations. The absorption and emission of a specified number of Tb^{3+} ions in a fluoride glass layer or plate is calculated on the basis of literature data. It is presumed that such a plate is placed in front of the solar cell and modifies the solar spectrum falling on the cell. This modified solar spectrum is used to calculate the efficiency of two model solar cells, an amorphous silicon and a microcrystalline silicon one, using the program Afors-Het 2.2. The amount of Tb^{3+} ions per unit area in the wavelength converter layer is varied. In the best case the efficiency of the a-Si:H solar cell improves by 1% and that of the microcrystalline silicon cell by 2.3%, in comparison to that calculated with the unmodified AM 1.5 spectrum.

M. Sendova-Vassileva (✉)
Central Laboratory of Solar Energy and New Energy Sources, Bulgarian Academy of Sciences, 1784 Sofia, Bulgaria
e-mail: marushka@phys.bas.bg

Introduction

As a way to achieve higher efficiency of third generation solar cells wavelength converters have been proposed as one of the ways forward [1]. The idea is to shift the wavelength of the light which is absorbed by the solar cell to the spectral region where the device is most efficient. Higher energy photons are often absorbed unproductively near the front contact of the solar cells or the carriers generated by them recombine before being separated. By the application of photoluminescent materials these photons are transformed into longer wavelength ones, which correspond to the spectral region of maximum efficiency for the solar cell and contribute more effectively to the generated photocurrent. The applicability of such an approach using quantum dots in a polymer layer has been demonstrated by van Sark et al. [2]. That wavelength converter was useful for multicrystalline silicon solar cells but did not show any improvement in the efficiency of amorphous silicon ones.

Another class of systems showing promise for application as wavelength converters are transparent layers containing rare earth ions such as Eu^{2+} [3], Eu^{3+} [4, 5], Sm^{2+} and Sm^{3+} [6], Tb^{3+} [4, 7], Nd^{3+} and Yb^{3+} [8]. The same principle is used in phosphor converted white light-emitting diodes to convert the UV or blue radiation into the visible [9]. These ions absorb in the blue and ultraviolet part of the spectrum and emit in the visible or near infrared. They are known to have high luminescence quantum efficiency (LQE) when excited but their absorption due to internal $4f^N$ transitions is low [1]. It is of great practical interest to estimate the degree to which rare earth ion based wavelength converters can increase the efficiency of solar cells as the reported experimental results vary quite widely [1, 7].

A rare earth ion that has been proposed as suitable for such application to thin film silicon solar cells is Tb^{3+} [4, 10]. In the present study the efficiency improvement in silicon-based thin film solar cells that could be expected by the application of a wavelength converter containing Tb^{3+} is estimated. Using literature data the spectral position and intensity of Tb^{3+} absorption and emission is calculated. Then the modification of the standard AM 1.5 solar spectrum produced by its passing through a transparent wavelength conversion layer or plate containing different amounts of Tb^{3+} ions is evaluated. The effect of that modified spectrum on the performance of model thin film silicon solar cells is estimated using the one-dimensional solar cell simulation program Afors-Het2.2 [11, 12].

Methods

The absorption spectrum of Tb^{3+} in a transparent glass matrix originating from transitions between electronic states in the partly filled 4f orbital is calculated according to the Judd–Ofelt theory [13, 14]. It is taken into account that the energy positions of the $4f^N$ transitions depend only weakly on the host matrix. Just the electric dipole contribution is included as it is the predominant one. The magnetic dipole oscillator strengths are much weaker. The electric dipole line strengths S_{ed} are evaluated according to the formula

$$S_{ed} = \left(\frac{e^2}{4\pi\varepsilon_0}\right) \sum_{\lambda=2,4,6} \Omega_\lambda \left\| U^{(\lambda)} \right\|^2 \quad (1)$$

where e and ε_0 have their usual meaning of unit charge and permittivity of vacuum, $\left\| U^{(\lambda)} \right\|$ are the reduced matrix elements of the unit tensor operator U. These matrix elements are commonly assumed to be independent of the host matrix [15]. Their values are taken from the work of Carnall et al. [16]. The Judd–Ofelt parameters Ω_2, Ω_4, Ω_6 are the host-dependent quantities in this model and they can be used to predict the electric dipole oscillator strengths for all radiative transitions between 4f levels. In our calculation we use the parameters for Tb^{3+} determined by Amaranath et al. [17] for the fluoride glass designated in the same paper as Glass A and having the composition $30BaF_2 + 30InF_3 + 10ThF_4 + 9ZnF_4 + 20LiF + 1TbF_3$. These parameters, shown in Table 1, are sufficiently high in value to give an optimistic estimation of the oscillator strengths of the optical transitions of the ion.

Table 1 Values of the Judd–Ofelt parameters used in the calculations [17]

Parameter:	Ω_2	Ω_4	Ω_6
Value $\times 10^{20}$ cm^2:	13.40	2.15	4.90

The oscillator strength of each transition is calculated as [15]:

$$f_{calc-ed} = 4\pi\varepsilon_0 \frac{8\pi^2 m\nu}{3h(2J+1)e^2} \chi_{ed} S_{ed} \quad (2)$$

where $\chi_{ed} = (n^2 + 2)^2/9n$, n is the refractive index of the matrix ($n = 1.57$ for Glass A [17]), J the quantum number of the total angular momentum of the ground level, ν the frequency of the transition, m the electron mass and h the Planck constant. The integral over each absorption band is connected with the oscillator strength:

$$\int \sigma_A(\nu) d\nu = \frac{\pi e^2}{4\pi\varepsilon_0 mc} f_{calc-ed} \quad (3)$$

where $\sigma_A(\nu)$ is the absorption cross-section of a single ion. This quantity multiplied by the number of ions per unit volume, N, gives the absorption coefficient, α.

Optical absorption at wavelengths shorter than 300 nm, where besides the internal $4f^N$ ones, transitions to $4f^{N-1}5d$ levels are observed, is not taken into consideration as these wavelengths do not form part of the solar spectrum reaching the earth and utilised by a solar cell on the earth's surface.

As a result we obtain the following absorption coefficient for 1×10^{21} ions/cm^3 Tb^{3+} in fluoride glass (Fig. 1). The intensities are calculated with a step of 5 nm to make them suitable for use by the solar cell simulation program. The spectrum is modelled in such a way that the integral over the spectral region remains equal to the sum of integrals of type (3) for all the absorption lines between 300 and 1200 nm. At the same time the spectral distribution of intensities corresponds to the ones of the calculated absorption lines.

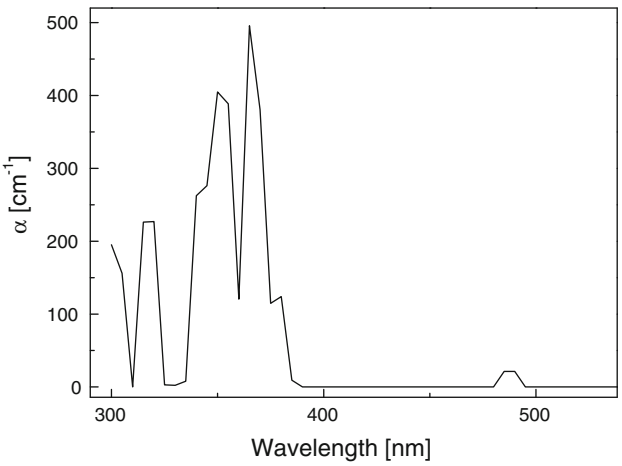

Fig. 1 Calculated absorption coefficient for 1×10^{21} ions/cm^3 Tb^{3+} in fluoride glass

In order to calculate the emission spectrum of Tb^{3+} ions in a transparent matrix irradiated with the AM 1.5 solar spectrum we implement the following procedure. First we calculate how many photons from the falling solar spectrum per second per unit area are absorbed in each Tb^{3+} absorption line, which is within the wavelength range of that solar spectrum. For this purpose we use the above absorption cross-section and the number of Tb^{3+} ions per square centimetre in the wavelength converter layer or plate we want to assess. In this way the number of ions per square centimetre of the device excited to a given $4f^N$ level of Tb^{3+} per second are calculated. Tb^{3+} has two emission levels—$^5D_3$ (26,800 cm^{-1}) and $^5D_4$ (20,500 cm^{-1}) (Fig. 2). All electrons excited to levels above the $^5D_3$ level thermalize by non-radiative transitions to that level as the energy gaps between them are small (process 1 in Fig. 2).

The spontaneous radiative emission rate from level a to level b is given by [15]:

$$A_{ab} = \frac{64\pi^4 \nu^3}{3hc^3(2J+1)} \chi'_{\mathrm{ed}} S_{\mathrm{ed}} \tag{4}$$

where $\chi'_{\mathrm{ed}} = n(n^2+2)^2/9$, J the quantum number of the total angular momentum of the initial level a, ν the frequency of the transition. S_{ed} are the line strengths calculated using (1), the Judd–Ofelt parameters in Table 1 and the reduced matrix elements for the radiative transitions of the Tb^{3+} ion given by Kaminskii [18].

The branching ratio β_{ab} for the radiative transition from a level a to a lower lying level b is given by [15]:

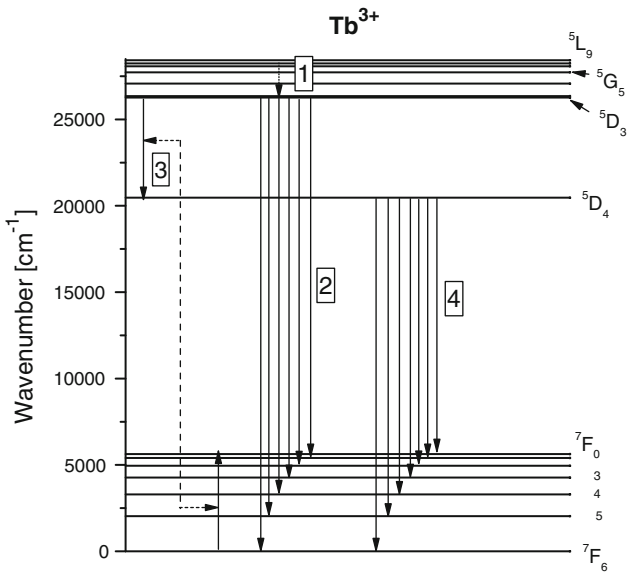

Fig. 2 Energy level diagram of Tb^{3+}. The *dotted arrow* illustrates the non-radiative transitions to the $^5D_3$ level. The *solid arrows* indicate the radiative transitions. On the *left side the long dash line* illustrates the resonant cross-relaxation process that takes place between neighbouring Tb^{3+} ions. The *numbers* point to the different relaxation processes as described in the text

$$\beta_{ab} = \frac{A_{ab}}{\sum_b A_{ab}} \tag{5}$$

where the sum in the denominator is over all lower lying levels. For the $^5D_4$ level b denotes the ^7F_J ($J = 6,5,4,3,2,1,0$) levels (Fig. 2). For the $^5D_3$ level the sum is over the same ^7F_J levels plus the $^5D_4$ level to which there is a small but finite spontaneous radiative emission rate. There is another channel for populating the lower $^5D_4$ level of Tb^{3+} at the expense of the higher $^5D_3$ one—cross-relaxation with a nearby ion in the ground state during which the energy of the $^5D_3 \rightarrow {}^5D_4$ transition is transferred to the $^7F_6 \rightarrow {}^7F_0$ transition of the unexcited ion as the energies of these two transitions are practically equal. In [19] the intensity ratio between the green photoluminescence (PL) originating from the $^5D_4$ level and the blue PL originating from the $^5D_3$ level for 1 mol% Tb is measured to be 3.9. This is the ratio we use in our calculations. To achieve this we presume a branching ratio of 0.7 for the resonant cross-relaxation process which transfers electrons from the $^5D_3$ to the $^5D_4$ level.

$$\beta_{\mathrm{CR}} = \frac{W_{\mathrm{CR}}}{W_{\mathrm{CR}} + \sum_b A_{ab}} = 0.7 \tag{6}$$

where W_{CR} is the resonant cross-relaxation rate.

In our model we presume that the Tb concentration is lower than that above which the PL intensity begins to fall because of concentration quenching. In different publications this value varies. For example, as demonstrated in [19–21] appreciable concentration quenching sets in above 1–5 mol% Tb^{3+}, which would mean above 10^{21} ions/cm^3 depending on the material, or distances between the Tb^{3+} of less than 10 Å. In our calculation we presume lower concentrations of Tb^{3+}, which for the three densities per unit area used would mean luminescent plates of less than 3 mm thickness.

The calculated number of excited ions to each level returns to the ground state by a series of non-radiative (1 in Fig. 2) and radiative (2 in Fig. 2) or cross-relaxation (3 in Fig. 2) and radiative (4 in Fig. 2) transitions according to the corresponding branching ratios. The emitted photons per second in all directions from a unit area of a layer containing 7×10^{18} ions/cm^2 Tb^{3+} (which could be, for example, 70 μm thick with a concentration of Tb 1×10^{21} ions/cm^2) and irradiated with the AM 1.5 solar spectrum have the spectral distribution shown in Fig. 3. It is calculated in the way described above with a presumed quantum efficiency of the fluorescence of 1. In fact the LQE of the Tb^{3+} emission measured at room temperature in [17] is 0.672 and in our calculations we use either this as the value for the LQE or LQE = 1 for comparison. The intensities are calculated with a step of 5 nm to make them suitable for use by the solar cell modelling program.

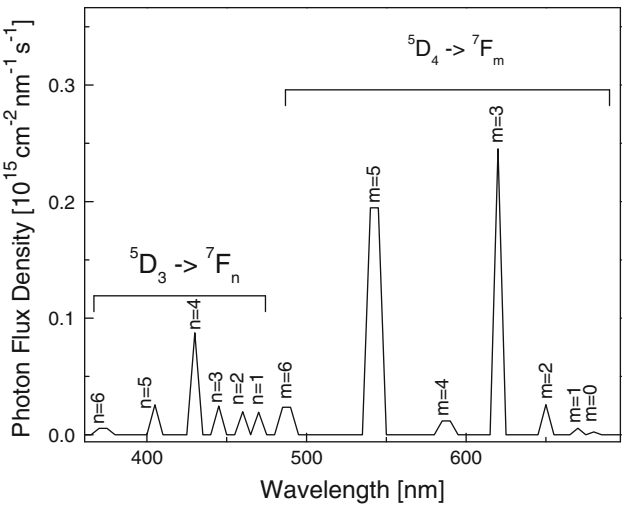

Fig. 3 Spectral distribution of emitted photons per second from a unit area of a layer containing 7×10^{18} ions/cm^2 Tb^{3+} ions, calculated in the way described in the text for LQE = 1. The radiative transitions are indicated in the figure

For the purpose of testing the influence of a wavelength converter containing Tb^{3+} ions on the performance of thin film solar cells the following scheme is used. We suppose that a glass layer or plate containing these ions has been placed in front of a thin film solar cell. The solar AM 1.5 spectrum passes through this glass layer and is modified by the absorption and emission of the rare earth ions in it. The modified spectrum (Fig. 4) falls on the solar cell and we calculate the cell's *J–V* characteristics using this modified spectrum. This approach is similar to the one used in [2]. According to the analysis made in [6] taking into account the refractive index of the fluorescent glass plate ($n = 1.57$) the fraction of photons emitted by the Tb^{3+} ions which falls on the front window of the thin film solar cell is 0.885. This analysis takes into account the fact that the PL is emitted spherically in all directions and part of it escapes at the top interface with air of the fluorescent plate depending on the incidence angle, part of it is reflected back towards the cell and some of the light propagating in the direction of the cell is reflected back by the interface. We use this coefficient in all our calculations.

The model cells used for estimating the effect of Tb^{3+} as a wavelength converter are two: an amorphous silicon and a microcrystalline silicon pin solar cell. The amorphous silicon pin cell is similar to the one used in [2] consisting of glass/TCO/*p* a-SiC:H/*i* a-Si:H/*n* a:Si:H/Ag, with layer thicknesses of 1 mm, 1 μm, 8, 500, 20 and 200 nm, respectively. The microcrystalline pin solar cell consists of glass/ZnO/*p* μc-Si:H/*p*/*i* μc-Si:H/*i* μc-Si:H/*n* a:Si:H/Ag [22], with layer thicknesses of 1 mm, 70, 30, 10, 800, 15 and 200 nm, respectively. Both solar cells are modelled with the program Afors-Het 2.2 [11, 12].

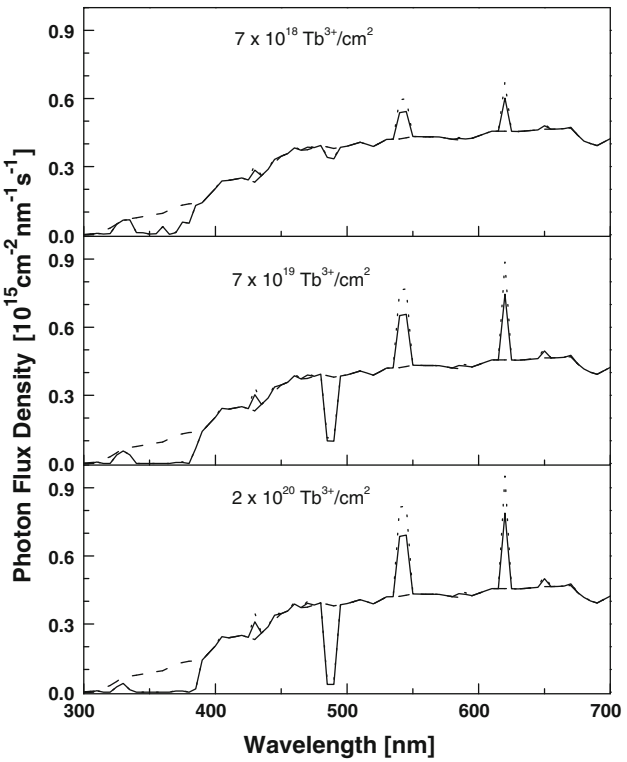

Fig. 4 Solar spectrum modified by the absorption and emission of a glass layer with the number of Tb^{3+} ions per unit area as indicated in the figure. The *dashed line* is the AM 1.5 spectrum, the *solid line* is the modified spectrum at LQE = 0.672, and the *dotted line* is the modified spectrum at LQE = 1

The program Afors-Het 2.2 (Automat FOR Simulation of HETerostructures) is a numerical simulation tool, which makes it possible to model heterojunction semiconductor devices. It was developed at the Hahn-Meitner Institute in Berlin (HMI) [12] and is distributed free of charge. The program solves the one-dimensional semiconductor equations using Shockley–Read–Hall recombination statistics for thermodynamic equilibrium and for steady-state conditions under an external illumination and/or bias voltage. A solar cell can be modelled as a series of electrical and optical layers. Each layer has a number of parameters defined for it including a file containing data for the absorption and refraction coefficients of the material. The electrical layers are the silicon p, i and n layers and the optical ones are the glass substrate, the transparent conductive oxide and the back metal contact. In order to calculate the generation profile within the electrical layers, internal multiple reflections are considered. Within each layer, it can be specified whether these multiple reflections should be treated as coherent or non-coherent. The material parameters used for the modelling of the a-Si:H cell are standard ones supplied with Afors-Het 2.2 while those for the μc-Si:H cell are taken from the low crystalline volume fraction cell in [22].

Table 2 *J–V* parameters under AM 1.5 illumination of the model cells calculated with the Afors-Het 2.2 program

	a-Si:H	μc-Si:H
J_{sc} (mA/cm^2)	13.32	13.43
V_{oc} (mV)	980	593
FF (%)	80.2	69.65
η (%)	10.46	5.55

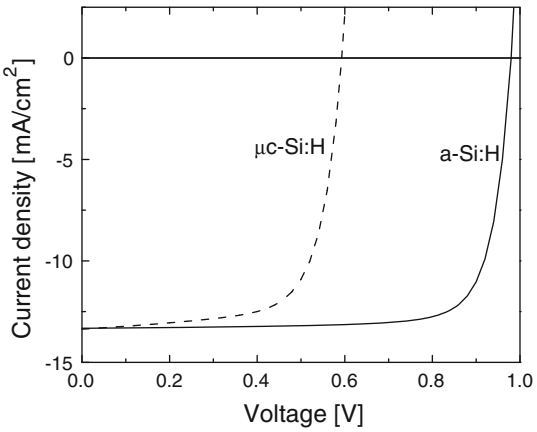

Fig. 5 Current–voltage characteristics of the two model thin film pin solar cells a-Si:H and μc-Si:H used for the calculation

The calculated *J–V* parameters for the two model cells under the standard AM 1.5 illumination are given in Table 2 and their *J–V* characteristics and quantum efficiency (QE) are shown in Figs. 5 and 6, respectively.

Results and discussion

The calculated results for the influence of the Tb^{3+} containing fluoride glass wavelength converter in front of each of the two model solar cells are shown in Tables 3 and 4, respectively. On the first line of each table the characteristics of the solar cell without any wavelength converter are shown. On the next lines the results of the calculations for increasing amounts of Tb^{3+} ions in the wavelength converter are presented. The evaluations are made for two LQEs of the Tb^{3+} ions as indicated above: for LQE = 1 in the first half of each table and LQE = 0.672 in the second half. The application of the wavelength converter has an effect primarily on the short circuit current (J_{sc}) of the solar cell, the open circuit voltage (V_{oc}) and the fill factor (FF) stay practically the same. When there is an increase in J_{sc} this leads to a higher efficiency and vice versa.

For the amorphous silicon cell (Table 3) there is a small 1% relative increase in the J_{sc} and the efficiency (η) only for LQE = 1. It does not depend on the amount of Tb^{3+} ions in the wavelength converter and remains the same for the three quantities studied. In the more realistic case of LQE = 0.672 there is no effect for the lowest Tb^{3+} concentration and a net decrease in efficiency for the two higher concentrations. The reasons for this are discussed below.

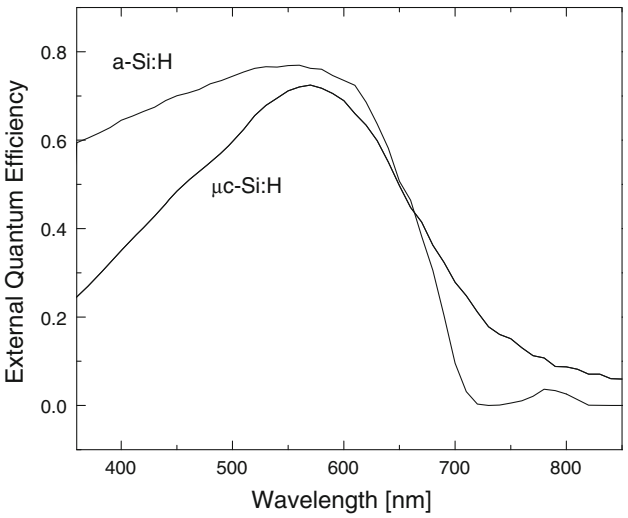

Fig. 6 Quantum efficiency of the two model thin film pin solar cells a-Si:H and μc-Si:H used for the calculation

For the microcrystalline silicon solar cell (Table 4) there is a concentration-dependent increase in the J_{sc} and the efficiency at LQE = 1. There is a slight increase of efficiency even at LQE = 0.672 but it is very small and decreases with Tb^{3+} concentration. At LQE = 1 the relative increase in efficiency reaches about 2.3% in the best case.

The short circuit current that could be generated if all photons in the AM 1.5 solar spectrum between 300 and 390 nm, where the Tb^{3+} ions absorb (Fig. 1) are wavelength converted to longer wavelengths and productively absorbed by the solar cell, is 1.1 mA/cm^2. However, the wavelength shifted photons are emitted with the corresponding LQE as explained above, which in most cases is lower than 1. Next it should be taken into account that the Tb^{3+} PL is emitted in all directions and due to the reflection by the surfaces of the fluorescent glass plate only a 0.885 fraction of these photons are incident on the solar cell. They are converted into electrical current with wavelength dependent QE as shown in Fig. 6, which again is well below unity. So the actual expected additional J_{sc} is much smaller.

On the other hand, as can be seen in Fig. 4 the amount of absorbed photons in the region 300–390 nm begins to saturate at the second amount of Tb^{3+} (7×10^{19} ions/cm^2) as there simply are no more photons available. So the number of wavelength shifted photons is not proportional to the amount of Tb^{3+} in the plate but varies sublinearly. So the change in J_{sc} also saturates (Tables 3, 4).

Table 3 Results of the modelling of the a-Si:H cell illuminated with the AM 1.5 spectrum modified by different amounts of Tb^{3+} ions per unit area given in the first column

Tb^{3+} (ions/cm^2)	$J_{sc} \pm 0.02$ (mA/cm^2)	$V_{oc} \pm 2$ (mV)	$\eta \pm 0.02$ (%)	FF $\pm$ 0.2 (%)	Relative increase in efficiency (%)
0	13.32	980	10.46	80.2	–
7×10^{18} LQE = 1	13.46	980	10.57	80.1	1.05
7×10^{19} LQE = 1	13.45	980	10.55	80.1	0.86
2×10^{20} LQE = 1	13.46	980	10.56	80.1	0.95
7×10^{18} LQE = 0.672	13.31	980	10.45	80.1	−0.1
7×10^{19} LQE = 0.672	13.16	980	10.33	80.1	−1.2
2×10^{20} LQE = 0.672	13.13	979	10.30	80.1	−1.5

Table 4 Results of the modelling of the μc-Si:H cell illuminated with the AM 1.5 spectrum modified by different amounts of Tb^{3+} ions per unit area given in the first column

Tb^{3+} (ions/cm^2)	$J_{sc} \pm 0.02$ (mA/cm^2)	$V_{oc} \pm 1$ (mV)	$\eta \pm 0.01$ (%)	FF $\pm$ 0.1 (%)	Relative increase in efficiency (%)
0	13.43	593	5.55	69.65	–
7×10^{18} LQE = 1	13.62	594	5.635	69.7	1.2
7×10^{19} LQE = 1	13.68	594	5.67	69.7	2.0
2×10^{20} LQE = 1	13.71	594	5.68	69.75	2.2
7×10^{18} LQE = 0.672	13.49	594	5.58	69.7	0.54
7×10^{19} LQE = 0.672	13.44	594	5.565	69.8	0.36
2×10^{20} LQE = 0.672	13.43	594	5.56	69.8	0.0

Besides it should be noted that in the wavelength range 360–390 nm the a-Si:H solar cell has QE approximately 60% and the wavelength conversion of phonons in this range probably does not lead to their more effective utilisation by the solar cell. Maybe this is the cause of the actual fall in efficiency for the a-Si:H solar cell in the case of LQE = 0.672. An argument for this is the fact that the fall in efficiency increases with the amount of Tb^{3+} in the plate, i.e. with the absorption in the short wavelength region (Table 3). A similar consideration is true for both cells, a-Si:H and μc-Si:H one, for the photons absorbed at 488 nm ($^7F_6 \rightarrow {}^5D_4$ transition) (Fig. 4) where the quantum efficiencies of the cells are good and the photons are wavelength converted with efficiency of less than 1 to longer wavelengths where the QE of the cells is not that much greater (difference of 5–10%).

The fact that the a-Si:H solar cell sees less improvement by the Tb^{3+} wavelength converter than the μc-Si:H one is due to its better QE in the blue part of the spectrum.

The combination of the factors mentioned above is reflected in the calculation results presented in Tables 3 and 4. From the data it can be inferred that the increase in solar cell efficiency due to the use of Tb^{3+} wavelength converters is small or non-existent. With the highest number of Tb^{3+} ions studied practically all the falling radiation in the spectral region where these ions absorb is converted so there is not more scope for improvement. In fact for the case of LQE = 0.672 and the higher numbers of Tb^{3+} ions per unit area (7×10^{19} ions/cm^2 for the a-Si:H cell and 2×10^{20} ions/cm^2 for both cells) the J_{sc} of the cells starts to fall in comparison with the lower Tb^{3+} amounts for the above-mentioned reasons. These results are comparable to those cited in Table 2 of [7] for the application of Tb^{3+} in a fluoride glass as a wavelength converter for a-Si solar cells and our experimental findings reported in [23].

The above considerations let us conclude that an ideal wavelength converter should not absorb in wavelength regions where the solar cell has a good efficiency and should emit with a high LQE at the peak of the QE of the cell to which it is applied.

Conclusions

The model calculations performed demonstrate that there is a very small increase in the efficiency of the studied thin film silicon solar cells when a transparent wavelength conversion layer or plate containing Tb^{3+} ions is placed in front of them. This improvement is limited to a 0.1% addition to the efficiency of each cell studied or a relative efficiency increase of 1 and 2.3% for the a-Si:H and the μc-Si:H cell, respectively. And this is only true when the LQE is presumed to be near unity. As most of the falling radiation in the wavelength region where the Tb^{3+} ion absorbs is converted at the highest Tb concentration studied, a much better performance for this combination of rare earth ion and type of solar cells could not be expected.

Comparison with the experimental data in the literature for this kind of ion confirms these findings.

References

1. Klampaftis E, Ross D, McIntosh KR, Richards BS (2009) Sol Energy Mater Sol Cells 93:1182
2. van Sark WGJHM, Meijerink A, Schropp REI, van Roosmalen JAM, Lysen EH (2005) Sol Energy Mater Sol Cells 87:395
3. Nakata R, Hashimoto N, Kawano K (1996) Jpn J Appl Phys 35:L90
4. Le Donne A, Acciarri M, Binetti S, Marchionna S, Narducci D, Rotta D (2008) In: Proceedings of the 23rd European photovoltaic solar energy conference, Valencia, Spain, pp 269–271
5. Fukuda T, Kato S, Kin E, Okaniwa K, Morikawa H, Honda Z, Kamata N (2009) Opt Mater 32:22
6. Hong B-C, Kawano K (2003) Sol Energy Mater Sol Cells 80:417
7. Kawano K, Hong BC, Sakamoto K, Tsuboi T, Seo HJ (2009) Opt Mater 31:1353
8. Rowan B, Richards BS, Robertson N, Jones A, Richardson P, Moudam O (2008) In: Proceedings of the 23rd European photovoltaic solar energy conference, Valencia, Spain, pp 700–703
9. He X-H, Lian N, Sun J-H, Guan M-Y (2009) J Mater Sci 44:4763. doi:10.1007/s10853-009-3668-4
10. Sendova-Vassileva M, Nikolaeva M, Angelov O, Vuchkov A, Dimova-Malinovska D, Pivin JC (2002) In: Marshall JM, Dimova-Malinovska D (eds) Photovoltaic and photoactive materials—properties, technology and applications, vol 80. Proc. NATO Advanced Study Institute, NATO Science Series II. Mathematics, Physics and Chemistry, Kluwer, Dordrecht
11. Stangl R, Kriegel M, Schmidt M (2006) In: Proceedings of WCPEC-4, 4th world conference on photovoltaic energy conversion, Hawaii, USA, May 2006
12. AFORS-HET: numerical simulation of solar cells and measurements. http://www.helmholtz-berlin.de/forschung/enma/si-pv/projekte/asicsi/afors-het/index_en.html. Accessed 12 Dec 2010
13. Judd BR (1962) Phys Rev 127:750
14. Ofelt GS (1962) J Chem Phys 37:511
15. Caspary R, Unrau UB (1998) In: Hewak D (ed) Spectroscopy of holmium-doped halide glass, properties, processing and applications of glass and rare earth-doped glasses for optical fibres. EMIS Group. Institution of Electrical Engineers. INSPEC, London
16. Carnall WT, Fields PR, Rajnak K (1968) J Chem Phys 49:4447
17. Amaranath G, Buddhudu S, Bryant FJ (1990) J Non-Cryst Solids 122:66
18. Kaminskii AA (1996) Crystalline lasers: physical properties and operating schemes. CRC Press, Boca Raton
19. Kam CH, Buddhudu S (2007) Phys B 337:237
20. Jia PY, Lin J, Yu M (2007) J Lumin 122–123:134
21. Hayakawa T, Kamata N, Yamada K (1996) J Lumin 68:179
22. Nath M, Roca i Cabarrocas P, Johnson EV, Abramov A, Chatterjee P (2008) Thin Solid Films 516:6974
23. Baumgartner K, Ahrens B, Angelov O, Sendova-Vassileva M, Dimova-Malinovska D, Holländer B, Schweizer S, Carius R (2010) In: Proceedings of 25th European photovoltaic solar energy conference and exhibition, Valncia, Sept 2010, pp 245–250